SYNTHESIS AND FUNCTIONALIZATION OF MAGNETIC NANOPARTICLES WITH POSSIBLE APPLICATION IN DRUG DELIVERY SYSTEMS

A. M. COJOCARIU, A. DOAGA, W. AMIN[a], P. BENDER[b],
R. HEMPELMANN[b], O. F. CALTUN[*]
Faculty of Physics and Carpath Center, Alexandru Ioan Cuza University, Bd. Carol I. Nr. 11, Iasi, 700506 Romania
[a]*Physical Chemistry, Saarland University, 66123 Saarbrücken, Germany*
[b]*Experimental Physics, Saarland University, 66123 Saarbrücken, Germany*

The present study consists in the preparation, characterization and functionalization of $Zn_xMn_{1-x}Fe_2O_4$ (x=0, 0.2, 0.4, 0.6, 0.8, 1) ferrite nanoparticles. The nanoparticles were prepared by co-precipitation method and were characterized by X-ray diffraction, transmission electron microscopy, ζ-potential, vibrating sample magnetometer and Fourier transform infrared measurements. The crystallite dimensions were calculated using the Scherrer formula and these were found in the range of 7 to 22nm. The micrographs indicate that the average size of particles has a value of 9nm for the $ZnFe_2O_4$ and increases until 23nm for the $MnFe_2O_4$ ferrite. The values obtained for ζ-potential confirmed the magnetic nanoparticles stability. The saturation magnetization increases proportional with manganese concentration having a maximum value of 67.7emu/g in the case of $MnFe_2O_4$. The functionalization of the nanoparticles was achieved with oppositely charged biocompatible polyelectrolytes (polyallylamine hydrochloride and pollyacrylic acid) using the layer-by-layer technique. After coating with each layer, measurements of ζ-potential and Fourier transform infrared spectroscopy has been performed in order to confirm the binding between the polyelectrolytes and magnetic nanoparticles.

1. Introduction

Nanotechnology represents the manipulation of matter on atomic and molecular scale. Due to these unique characteristics nanotechnology is applied in various fields such as physics, chemistry, engineering or medicine. In medicine, nanoparticles offer the opportunity to create multifunctionality with potential in innovating diagnosis and therapeutic modalities for a number of diseases [1]. The use of particles of nanometric order has become interesting for researchers in cancer therapies due to their properties: they posed high surface-to-volume ratios making possible the modification with different surface functional groups and they also have minimal renal filtration [2]. In diagnosis, nanoparticles can be used as contrast agents in magnetic resonance imaging (MRI) [3, 4] after determining their quality by particle magnetic properties, particle size distribution and particle surface charge. Hyperthermia and drug delivery became two of the most important research fields for applications of nanoparticles in cancer therapies. Hyperthermia procedure with magnetic nanoparticles offers the possibility to induce extra heat to local area through the oscillation of the magnetic moment inside the nanoparticles [5]. In pharmacotherapy the interest is to deliver the optimum amount of drug to a specific location inside the body, to maintain it there for a suitable period of time [6], minimizing the side effects over the healthy

---

[*]Corresponding author: caltun @uaic.ro

tissues.

Due to the requirements for biocompatibility and biodegradability, magnetic nanoparticles need to be coated before medical usage. The coating of nanoparticles produces changes in physicochemical properties by modifying the functionalities, charges and the reactivity of the surface.

The group of Decher in 1992 [7] used synthetic polyelectrolytes that were successively layered onto a substrate by electrostatic interactions. This technique is based on the use of different polyelectrolytes (polyethyleneimine, polyallylamine hydrochloride, polystyrenesulfonate, polyvinylsulfate and polyacrylic acid) of opposite charges. In 1999, Caruso et al. [8] were the first who presented the possibility of layer-by-layer (LbL) technique to functionalize nanoparticles that don't exceed 100nm while limiting aggregation.

For the first time the LbL technique was used to functionalize a complete series of $Zn_xMn_{1-x}Fe_2O_4$ (x=0, 0.2, 0.4, 0.6, 0.8, 1) ferrite synthetized by co-precipitation method. The ferrite composition series has been chosen because it involves only biocompatible non-toxic metal ions and due to their applicability as possible MRI contrast agents [9, 10], drug delivery carriers [11] and in hyperthermia process [12].

2. Experimental details

2.1 Chemicals

The chemicals used for the preparation and functionalization of $Zn_xMn_{1-x}Fe_2O_4$ ferrite nanoparticles were: NaOH (ROTH GmbH, Germany), Fe $(NO_3)_3•9H_2O$ (AppliChem), $FeCl_3•6H_2O$ (Sigma-Aldrich Laboratory), $ZnCl_2$ (ROTH GmbH, Germany), $MnCl_2$ (Aldrich), HNO_3 (BDH PROLABO), HCl (Zentralis Chemie Labor), trisodium citrate dehydrate (BDH PROLABO), Polyallylamine hydrochloride (Sigma Aldrich Laboratory) and Polyacrilic acid (Sigma Aldrich Laboratory).

2.2 Synthesis details

When referring to the synthesis method it is necessary to specify that although there are different methods available, each one presents both advantages as well as disadvantages. In terms of size and morphology control of magnetic nanoparticles, thermal decomposition [13] and hydrothermal synthetic route [14] represents the optimal method. In order to obtain water-soluble and biocompatible magnetic nanoparticles, co-precipitation [15] was often employed although this method has a lower control of the particle shape, broad distribution of sizes and aggregation of particles. Besides the advantages already presented, co-precipitation represents an easy, economical and simple method to produce magnetic nanoparticles.

This study was focused on the preparation, characterization and functionalization of $Zn_xMn_{1-x}Fe_2O_4$ ferrite nanoparticles with x = 0, 0.2, 0.4, 0.6, 0.8 and 1. The magnetic nanoparticles have been prepared by the co-precipitation technique. In the first step, 200mL of 0.25M NaOH was kept under continuous stirring until the temperature of 90^oC was reached. Meanwhile, a 40mL solution 0.04 mol $FeCl_3•6H_2O$ was heated up to 70^oC and then mixed with a solution of X mol of $ZnCl_2$ and Y mol $MnCl_2$ dissolved in 8mL water. The dark coloured suspension that formed was kept under stirring for 1h at 90^oC and then left to cool for another hour. The suspension was washed three times with water. In order to stabilize the nanoparticles 2M HNO_3 was added [16]. At the same time, a solution of 8.5mL containing X/2 mol of $ZnCl_2$ and Y/2 mol of $MnCl_2$ was added to 60mL solution of 0.02 $Fe(NO_3)_3·9H_2O$. The solution was prepared at 70^oC. The resulted solution was added to the dark suspension that was formed and kept under stirring for 30min at 80^oC. The magnetic nanoparticles were washed three times in 200mL water using a permanent magnet for separation. For medical applications it is necessary to have a stable ferrofluid, and to this purpose the solution was kept under dialysis against 0.01M citrate solution for 7 days and then again for another 7 days to remove the excess of citrate. The values used for preparation of this series are listed in Table 1. All synthesized nanoparticles presented a pH between 6.7 -7.

*Table 1 Molar concentration values for different Zn substitution level of $Zn_xMn_{1-x}Fe_2O_4$
ferrite series*

Sample	Concentration (mol)		
	Zn^{2+}	Mn^{2+}	Fe^{3+}
$MnFe_2O_4$	-	0.02	0.04
$Zn_{0.2}Mn_{0.8}Fe_2O_4$	0.004	0.016	0.04
$Zn_{0.4}Mn_{0.6}Fe_2O_4$	0.008	0.012	0.04
$Zn_{0.6}Mn_{0.4}Fe_2O_4$	0.012	0.008	0.04
$Zn_{0.8}Mn_{0.2}Fe_2O_4$	0.016	0.004	0.04
$ZnFe_2O_4$	0.02	-	0.04

Layer-by-layer technique was used for the functionalization of the $Zn_xMn_{1-x}Fe_2O_4$ ferrite nanoparticles with x = 0, 0.2, 0.4, 0.6, 0.8 and 1. This technique uses oppositely charged polyelectrolytes from dilute aqueous solution which are consecutively deposited onto solid substrates by utilizing the electrostatic attraction and complex formation between polyanions and polycations [17]. The LbL technique used for surface-mediated drug delivery holds great potential, not only to modulate surface properties, but also as drug reservoir [18]. Polyallylamine hydrochloride (PAH) [18], which is a polycation, was used to coat the magnetic nanoparticles that posed a negative charge on the surface. Briefly, 9mL of magnetic nanoparticles were added to 9mL of aqueous solution that contains 25mg of PAH. The solution was kept under stirring in the dark for 6 hours at room temperature. The purification of the solution was made by dialysis against water for 2 days. The second layer, polyacrilic acid (PAA) [19], which plays the role of the polyanion, was deposited according to the previously described method. After the coating with the third layer, PAH, the nanoparticles were stored in the dark at 4°C.

2.3 Characterization techniques

A PANanalytical X'Pert Pro MPD X-ray diffractometer was used to determine the crystal structure of $Zn_xMn_{1-x}Fe_2O_4$ ferrite nanoparticles. The diffractograms were recorded using Cu-K$_\alpha$ radiation (λ=1.54Å), a power of 45kV, a current of 40mA at room temperature and a typical step size of 0.02^o. The estimation of the particles size is maid via Scherrer´s formula.

A JOEL Model JEM 2010 (JOEL GmbH, Eching Germany) transmission electron microscope, operating at an accelerating voltage of 200kV, is used to record TEM images. For each measurement a drop of the colloidal ferrite particles was deposited on a copper grid (D = 3mm). Vibrating sample magnetometer (VSM) Lake Shore Model 7300 is employed for room temperature *M-H* loops applying a field that varies between -2T and 2T. The uncoated particles were also analysed by using a Fourier transmission infrared spectrometer (Jasco 660 Plus) in KBr disk, in the range of 4000-400cm^{-1} with a resolution of 4cm^{-1}.

The presence of polyelectrolytes was confirmed by Fourier Transformed InfraRed spectroscopy (FTIR), recorded with a Perkin Elmer spectrometer between 500 and 4000cm^{-1} and by ζ-potential measurements, using a Zetasizer Nano ZS from Malvern Instruments.

3. Results and discussion

The structural study is essential for optimizing the properties needed for various applications. The phase identification was performed on an X-ray diffractometer. The XRD analyses of the $Zn_xMn_{1-x}Fe_2O_4$ (x=0, 0.2, 0.4, 0.6, 0.8, 1) ferrite nanoparticles (Figure 1) revealed the characteristic cubic spinel structure.

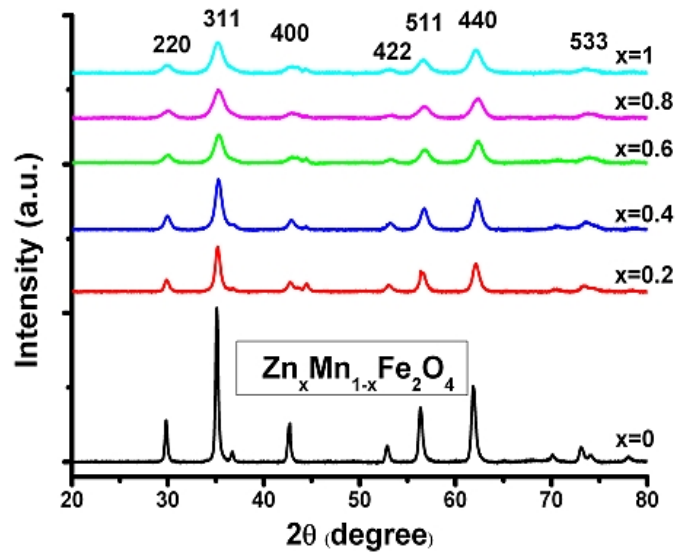*Fig. 1. X-ray diffraction patterns of $Zn_xMn_{1-x}Fe_2O_4$*

The crystallite size of $Zn_xMn_{1-x}Fe_2O_4$ (x= 0, 0.2, 0.4, 0.6, 0.8, and 1) ferrite was determined using Scherrer's equation:

$$D = k\lambda / \beta \cos\theta \qquad (1)$$

The X-ray wavelength of λ is 1.54 Å, the shape factor, k, is considered equal to 0.9, θ is the Bragg angle and β is the full width at half maximum in radians. To assess the crystallite size of the particles the half maximum width (FWHM) of the (311) X-ray diffraction line, for all the precipitated powder samples, was used. The crystallite size of $Zn_xMn_{1-x}Fe_2O_4$ dried precipitates can be found in Table 2.

Table 2 Crystallite size (D_{XRD}), particles diameter (D_{TEM}) and maximum magnetization (M_{max}) for $Zn_xMn_{1-x}Fe_2O_4$ ferrite nanoparticles

Sample	D_{XRD} (nm)	D_{TEM} (nm)	M_{max} (emu/g)
$MnFe_2O_4$	22	23	67.7
$Zn_{0.2}Mn_{0.8}Fe_2O_4$	14	16	60
$Zn_{0.4}Mn_{0.6}Fe_2O_4$	13	14	50
$Zn_{0.6}Mn_{0.4}Fe_2O_4$	10	12	33.4
$Zn_{0.8}Mn_{0.2}Fe_2O_4$	9	10	20.6
$ZnFe_2O_4$	7	9	20.7

The average crystallite size decreases from 22 to 7nm with increasing Zn concentration from x = 0 to x = 1. Arulmurugan et al. [20] reported that the zinc substitution plays an important role in reducing the particle size of the series. This can be explained by the fact that an increase in the zinc concentration in the solution increases the reaction rate, favoring the formation of the ultrafine particles.

The size and morphology of magnetic nanoparticles were characterized by transmission electron microscopy (TEM). The typical TEM micrographs of magnetic particles are shown in Figure 2. The average particle size was determined using ImageJ software, by measuring approximative

80 particles for each sample from the series. The reduction of particle size with the zinc concentration is evident in TEM micrographs. The dimensions of particles were found to be in the same range of nanometers as crystallite size estimated from XRD data (Table 2) suggesting single domain nanoparticles. The average particles dimensions present the same trend as the crystallite ones; it tends to increase with the manganese concentration.
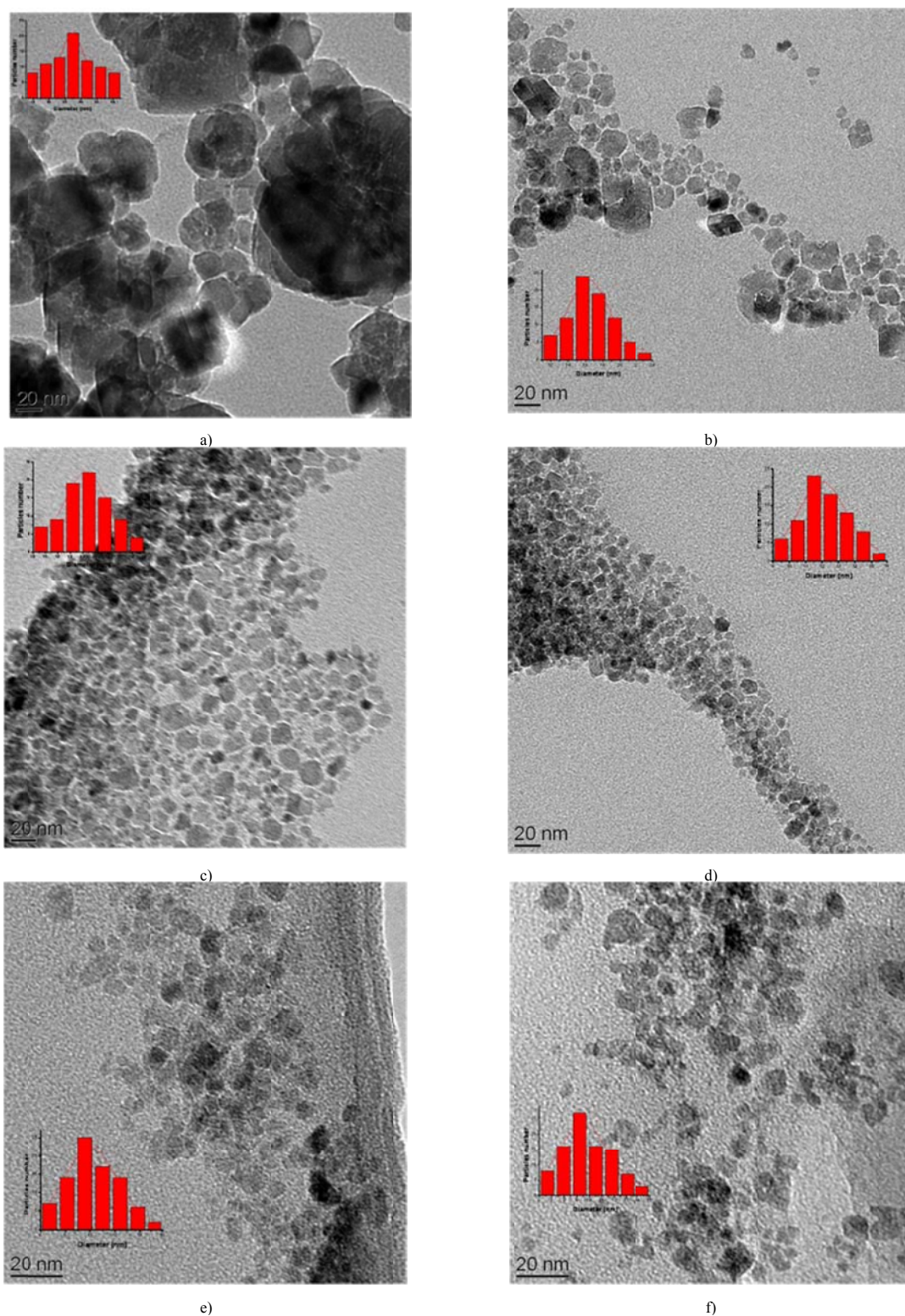

Fig. 2. TEM micrographs for $Zn_xMn_{1-x}Fe_2O_4$ where (a) $MnFe_2O_4$, (b) $Zn_{0.2}Mn_{0.8}Fe_2O_4$, (c) $Zn_{0.4}Mn_{0.6}Fe_2O_4$, (d) $Zn_{0.6}Mn_{0.4}Fe_2O_4$, (e) $Zn_{0.8}Mn_{0.2}Fe_2O_4$ and (f) $ZnFe_2O_4$ nanoparticles.

The magnetization curves of the nanoparticles of $Zn_xMn_{1-x}Fe_2O_4$ series, presented in Figure 3 have confirmed the superparamagnetic behavior of the as-synthesized powders. From the curves it can easily be observed that the magnetic properties of Zn-Mn ferrites are strongly dependent on the Zn concentration. The saturation magnetization decreases from 67.7emu/g registered for $MnFe_2O_4$ until 20.7emu/g for the $ZnFe_2O_4$. The values for the maximum magnetization of all series can be found in Table 3. Although it is well known that bulk $ZnFe_2O_4$ is a normal spinel that has antiferromagnetic properties below the Néel temperature of 10K, at room temperature behaves paramagnetic. According to Néel, small antiferromagnetic particles can exhibit superparamagnetism and weak ferromagnetism due to uncompensated spins in the two sublattices. Examining the magnetization curves, one can see that for x = 0.8 and x = 1 the saturation magnetization, around 20.6emu/g respectively 20.7emu/g, is higher compared with the reported value of approximate 5emu/g for the bulk $ZnFe_2O_4$. The superparamagnetic behaviour of these ferrites could be attributed to spin canting and surface spin disorder that occurred in these nanoparticles [21].
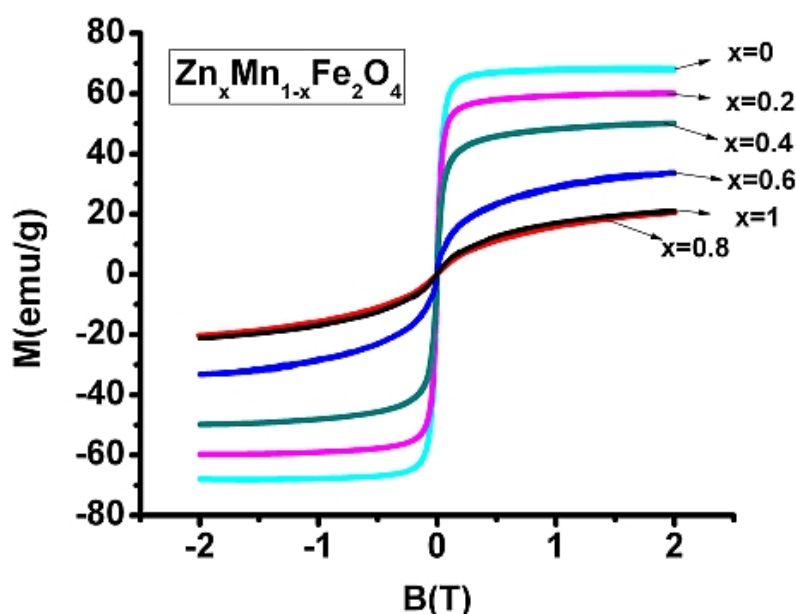

Fig. 3. Hysteresis loops of $Zn_xMn_{1-x}Fe_2O_4$ magnetic nanoparticles at room temperature; the missing hysteresis indicates that the nanoparticles indeed are superparamagnetic

Biomedical applications require the use of biocompatible nanoparticles. In order to achieve this requirement various self-assembly methods using polymers have received an increasing interest [22]. Due to both electrostatic and steric effects resulting from the PE coating, particles can either stabilize or agglomerate. The thickness of the polyelectrolyte coating can be increased by the additions of oppositely charged polyelectrolytes (PE). As it is known, the ζ-potential shows the potential difference between the dispersion medium and the stationary layer of fluid attached to the dispersed particle. Its significance relays in the fact that the resulted value can be related to the stability of colloidal dispersions. Measuring the ζ-potential after each step, one can observe the changes occurred in the surface charges, confirming this way the presence of the polyelectrolyte on the magnetic nanoparticle's surface and its degree of stability (Table 3).

Table 3 Values of the ζ-potential for the $Zn_xMn_{1-x}Fe_2O_4$ magnetic nanoparticles, before and after each coating step

Sample	ζ –potential (mV)uncoated nanoparticles	ζ –potential (mV)coated nanoparticles PAH	ζ –potential (mV) coated nanoparticles PAH/PAA	ζ –potential (mV) coated nanoparticles PAH/PAA/PAH
$MnFe_2O_4$	-47.7	+31.2	-37.8	+37
$Zn_{0.2}Mn_{0.8}Fe_2O_4$	-50	+39.6	-40.4	+43
$Zn_{0.4}Mn_{0.6}Fe_2O_4$	-42.3	+36.6	-39.6	+39.4
$Zn_{0.6}Mn_{0.4}Fe_2O_4$	-46.9	+38.9	-32.9	+37.2
$Zn_{0.8}Mn_{0.2}Fe_2O_4$	-52.2	+36.3	-38.2	+40.4
$ZnFe_2O_4$	-51.2	+43.6	-36.7	+37.8

Examining the spectra of the uncoated particles (Figure 4a) it can be observed an O–H strong absorption peak at around 3500cm^{-1} due to the physical adsorption of water. Also this spectra exhibit two vibrational bands, one located around 600cm^{-1} and the other ranged around 400cm^{-1} [23]. These two frequency bands correspond to the tetrahedral respectively octahedral sites, confirming this way the existence of the spinel structure.

FTIR has been widely used to confirm an attachment of different functional groups in each step of functionalization. Further evidence of the presence of the polyelectrolyte bound to the magnetic nanoparticles is provided by FTIR spectra as shown in Figure 4b. IR spectra of the coated magnetic nanoparticles confirmed the absorption of the first layer (PAH) on the surface of the magnetic nanoparticles.
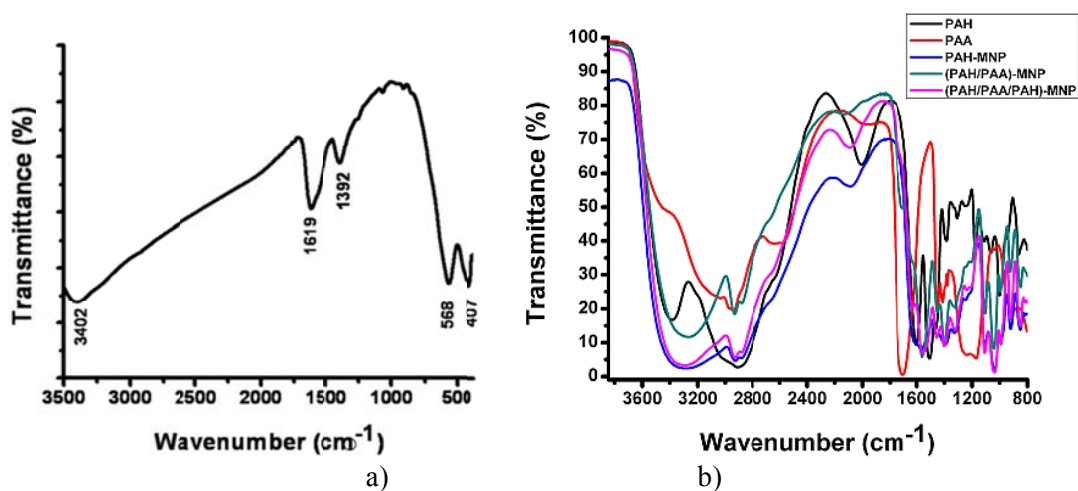

Fig. 4. Fourier transform infrared spectra of the magnetic nanoparticles after each polyelectrolyte deposition in comparison to the pure polyelectrolytes PAH and PAA.

The coresponding vibrations of the NH$_3^+$ group are found arround 1600cm^{-1} and 1500cm^{-1} wave numbers, representing asymmetric and symmetric deformation vibrations. The band located at 2000cm^{-1} corresponds to the stretching vibration of N-H$^+$ group. The peak that corresponds to the C-N stretching vibration was registered at the wave number 1000cm^{-1}. The presence of the second layer (PAA) was confirmed through the stretching vibration of the carboxyl group (C=O) around 1710cm^{-1} wave number, whereas the peaks corresponding to the asymmetric stretching vibration of the deprotonated carboxyl group (COO$^-$) present a weak signal around 1570cm^{-1}, that can be confused with the one from the NH$_3^+$ group [24, 25].

4. Conclusions

For the first time the synthesis, characterization and functionalization of the $Zn_xMn_{1-x}Fe_2O_4$ (x=0, 0.2, 0.4, 0.6, 0.8, 1) ferrite series has been purposed. Magnetic nanoparticles were synthesized by using co-precipitation chemical method. XRD analyses allowed determining the presence of characteristic spinel structure in the $Zn_xMn_{1-x}Fe_2O_4$ ferrofluid nanoparticles having crystallite size between 7 and 22nm. The size distribution of the magnetic nanoparticles determined by TEM is consistent with the crystallite size obtained from XRD measurements. The magnetization increased with increasing of the Mn concentration from 20.7 to 67.7emu/g. The presence of the polyelectrolyte on the magnetic nanoparticle's surface was confirmed by FTIR and ζ-potential measurements, the surface charge value changing after each step. The range of applications of these coatings varies, depending on the particles that are attached to the polyelectrolyte shell. Such applications include targeted therapy in cancer when the nanoparticles are coated with different antibodies directed against typical molecules on the surface of cancer cells. We have shown that the LbL technique used for polyelectrolyte deposition can be applied in order to achieve functionalization of $Zn_xMn_{1-x}Fe_2O_4$, x varying between 0 and 1, magnetic nanoparticles suitable for biomedical applications.

Acknowledgements

References

[1] T.J. Harris, G. Von Maltzahn, S.N. Bhatia, Nanotechnology for Cancer Therapy, Chapter 5: Multifuntional nanoparticles for Cancer Therapy, 2007 by Taylor & Francis Group, LLC

[2] S. Abdelmawala, S. Guo, L. Zhang, S.M. Pulukuri, P. Patankar, P. Conley, J. Trebley, P. Guo, Q.X. Li, Molecular Therapy **19**(7), 1312 (2011)

[3] J. Della Rocca and W. Lin, Eur. J. Inorg. Chem. 2010 (24), 3725 (2010)

[4] C.P. Constantin, T. Slatineanu, M. Palamaru, A. Iordan, O.F. Caltun, Digest Journal of Nanomaterials and Biostructures **7**(4), 1793 (2012)

[5] A. Chicheł, J. Skowronek, M. Kubaszewska, M. Kanikowski, Rep Pract Oncol Radiother **12**(5), 267 (2007)

[6] T. Neuberger, B. Schopf, H. Hofmann, M. Hofmann, B. von Rechenberg, J. Magn. Magn. Mater **293**, 483 (2005)

[7] G. Decher, J. D. Hong and J. Schmitt, Thin Solid Films 210/21 I, 831 (1992)

[8] F. Caruso, C. Schuler and D. G. Kurth, Chem. Mater.11, 3394 (1999)

[9] J. Lu, S. Ma, J. Sun, C. Xia, C. Liu, Z. Wang, X. Zhao, F. Gao, Q. Gong, B. Song, X. Shuai, H. Ai, Z. Gu, Biomaterials 30, 2919 (2009)

[10] C. Barcena, A. K. Sra, G. S. Chaubey, C. Khemtong, J. Ping Liu and J. Gao, Chem. Commun 2224 (2008)

[11] X. Le Guével, E.M. Prinz, R. Műller, R. Hempelmann, M. Schneider, J Nanopart Res **14**, 727 (2012)

[12] R. Valenzuela, Hindawi Publishing Corporation Physics Research International Vol. 2012, Article ID 591839

[13] S. Sun, H. Zeng, J. Am. Chem. Soc. **124**(28), 8204 (2002)

[14] Z. Jing, S. Wu, Mater. Lett. **58**, 3637 (2004)

[15] A. Figuerola, R. Di Corato, L. Manna, T. Pellegrino, Pharmacological Research **62**, 126 (2010)

[16] K. Mandel, W. Szczerba, A. Thnemann, H. Riesemeier, M. Girod, G. Sextl, J Nanopart Res

14, 1(2012)

[17] C. Gao, S. Leporatti, S. Moya, E. Donathand, H. Möhwald, Chem. Eur. J. **9**(4), 915 (2003)

[18] C.M. Jewell, D.M. Lynn, Curr. Opin. Colloid Interface Sci. **13**, 395 (2008).

[19] M. Delcea, H. Möhwald, A. G. Skirtach, Advanced Drug Delivery Reviews **63**, 730 (2011)

[20] R. Arulmurugan, B. Jeyadevan, G. Vaidyanathan, S. Sendhilnathan, J. Magn. Magn. Mater, **288**, 470 (2005)

[21] N. M. Deraz, A. Alarifi, Int. J. Electrochem. Sci. **7**, 6501 (2012)

[22] Ai H., Advanced Drug Delivery Reviews **63**, 772 (2011)

[23] A.M. Cojocariu, M. Soroceanu, L. Hrib, V. Nica, O.F. Caltun, Mater Chem Phys **135**, 728 (2012)

[24] Socrates G, Infrared and Raman characteristic group frequencies: tables and charts - 3rd edition, Wiley, 2004

[25] M.A. Mutar, N.D Radia, Iraqi National Journal of Chemistry **45**, 67 (2012)